NUMERICAL MODELLING OF THE SEASONAL VARIABILITY OF PLANKTON AND FORAGE FISH IN THE GULF OF KHAMBHAT

Vijay Kumar[1] and Girija Jayaraman[1,2]

1. Centre for Atmospheric Sciences, Indian Institute of Technology, Hauz Khas, New Delhi, India (vijayiitdelhi@gmail.com)
2. Department of Mathematics, The University of the West Indies, Mona, Kingston, Jamaica, West Indies

1. Abstract

Marine ecological modelling has to deal with a cascade of scales associated with physical and biological oceanographic processes. The range of space and time scales over which marine organisms exist is large and these scales overlap with a variety of physical scales. Representing the interaction of these processes at different spatial and temporal scales is of main concern towards the development of a model. Coupling circulation and biological processes in a single model could be quite challenging due to stiffness of the coupled system. The governing system of partial differential equations represents the interaction of the physical, biological and chemical processes in a marine environment.

Numerical modeling of marine ecology exploits several assumptions and it is indeed quite challenging to include marine ecological phenomena in to a mathematical framework. The key concern in the development of a numerical model is the categorization of compartment of species. It is nevertheless assumed that one particular model compartment contains the same type of marine species. In the present formulation, a five-compartment NPZDF (Nutrient, Phytoplankton, Zooplankton, Detritus, Forage Fish) model is formulated using advection-diffusion-biological equations in order to understand the ecological dynamics in the marine environment.

For the development and exploration of the model's behavior we have concentrated on the modeling of seasonal cycle in the Gulf of Khambhat (19º 48' N - 22º20' N, 65º E - 72º40' E). It has rich bio-diversity and a high productive area due to elevated turbidity and geographical location. The varying geography of Gulf of Khambhat is projected to a rectangular domain through co-ordinate transformations. Model simulated results agree well qualitatively with SeaWiFs and MODIS Aqua Chlorophyll data, pattern of peaks being nearly the same.

2. Study Area

Geographical location of study area is (19º 48' N - 22º20' N, 65º E - 72º40' E). It has irregular boundary and combination of two type of water body; i. Shallow water body near the coast and ii. Deep Ocean away from the coast (Figure 1).The Gulf of Khambhat receives annually 38 km3 freshwater and 74X109 kg of sediment from 12 tributary rivers, [Sinha et al., 2010, Jaiswar et. al., 20011, Deshkar et al., 2012]. The tidal currents are strong and bimodal in nature which brings bottom sediments in water column (*http://www.icmam.gov.in /GUK.PDF*). All these circumstances made high nutrient in the region of study area. Sea surface currents, bathymetry for shallow water and mixed layer for deep Ocean are used as a input in model. The input data are available on the website (*http://apdrc.soest.hawaii.edu/las/v6/constrain?var=328* and *http://las.Incois.gov.in/las/UI.vm*). Coordinate transformation are used for making irregular to regular boundary of domain of study area.

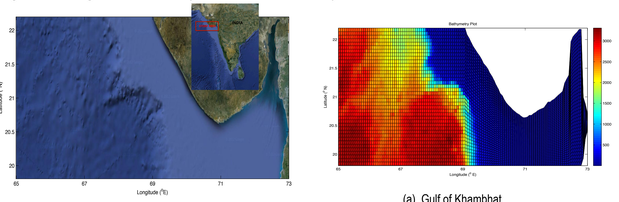

(a). Gulf of Khambhat

(a). Gulf of Khambhat

Figure 1. Study Area and Bathymetry

3. Methodology

Mathematical modelling of marine ecology is based on marine food web. Figure 2. shows a schematic diagram of the food web on which the present model is based.

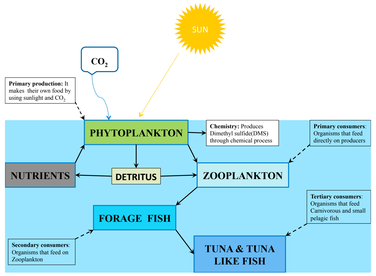

Figure 2. Schematic diagram for marine food web.

3.1 The variation of species in an aquatic Environment

$$\frac{\partial B}{\partial t} = \text{Transport} - \text{Loss} + \text{source}, \qquad \text{B=concentration of a biological tracer.}$$

Transport in the horizontal directions (x,y) is described by diffusion-advection equation. Loss term depends on the mortality rate of species. Source term is the biomass recruitment.

3.2 Governing Equations of model :

$$\frac{\partial N}{\partial t}+u\frac{\partial N}{\partial x}+v\frac{\partial N}{\partial y}=\sigma_x\frac{\partial^2 N}{\partial x^2}+\sigma_y\frac{\partial^2 N}{\partial y^2}-(\frac{\alpha(\phi,H,t)N}{K_N+N}-r)P+r_1D+\frac{m_0+\zeta^+(t)}{M(t)}(N_D-N)$$

$$\frac{\partial P}{\partial t}+u\frac{\partial P}{\partial x}+v\frac{\partial P}{\partial y}=\sigma_x\frac{\partial^2 P}{\partial x^2}+\sigma_y\frac{\partial^2 P}{\partial y^2}+(\frac{\alpha(\phi,M,t)N}{K_N+N}-r)P-\frac{p_1P}{A}(\frac{c(A-A_{Th})Z}{K_Z+(A-A_{Th})})-(\frac{\mu P}{k+P})P-\frac{m_0+\zeta^+(t)}{M(t)}P$$

$$\frac{\partial Z}{\partial t}+u\frac{\partial Z}{\partial x}+v\frac{\partial Z}{\partial y}=\sigma_x\frac{\partial^2 Z}{\partial x^2}+\sigma_y\frac{\partial^2 Z}{\partial y^2}+\frac{ec(A-A_{Th})Z}{K_Z+(A-A_{Th})}-\frac{\zeta(t)}{M(t)}Z-gZ$$

$$\frac{\partial D}{\partial t}+u\frac{\partial D}{\partial x}+v\frac{\partial D}{\partial y}=\sigma_x\frac{\partial^2 D}{\partial x^2}+\sigma_y\frac{\partial^2 D}{\partial y^2}+(\frac{\mu P}{k+P})P-r_1D+\frac{p_1P}{A}(\frac{(1-e)c(A-A_{th})Z}{K_Z+(A-A_{th})})-\frac{p_2D}{A}(\frac{ec(A-A_{th})Z}{K_Z+(A-A_{th})})$$

$$\frac{\partial F}{\partial t}+u\frac{\partial F}{\partial x}+v\frac{\partial F}{\partial y}=\sigma_x\frac{\partial^2 F}{\partial x^2}+\sigma_y\frac{\partial^2 F}{\partial y^2}-\lambda F+e^{m_r t_r}PP, \quad m_r=-\log(0.04/t_r),$$

3.3 Boundary Conditions :

$$\frac{\partial B}{\partial \eta}=0, \text{ at coastal boundary and } B(x,y,t)=B_0, \text{ at open Ocean, where } \eta \text{ is a unit vector}$$

4. Coordinate Transformation

To facilitate the numerical treatment of an irregular boundary configuration, a coordinate transformation (Figure 3) is introduced, which is based upon a new set of independent variables x and ξ, where

$$\xi(x,y)=\frac{y-b_1(x)}{b(x)},\ b(x)=b_2(x)-b_1(x)$$

This mapping transforms the analysis area into a rectangular domain given by 0 < x < L_x, 0 < ξ < 1. Thus the boundaries y=b_1(x) and y=b_2(x) correspond respectively to ξ=0 and ξ=1.

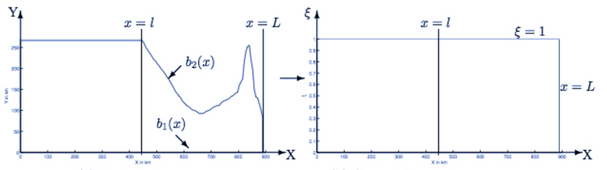

(a)Physical plane (b) Computational plane

Figure 3. Physical and computational domain

4.1 Grid Generations

(a).The discrete coordinate points for physical plain, shown in figure 4. a.

$$x_i=i\Delta x, \quad \text{for } i=0,\ 1,\ 2,\ 3,\ \ldots\ldots,m;\ \ \Delta x=\frac{L}{m},$$

$$y_j(i)=j\Delta y(i), \quad \text{for } j=0,\ 1,\ 2,\ 3,\ \ldots\ldots,n;\ \ \Delta y(i)=\frac{b(i)}{n},\ i=0,\ 1,\ 2,\ 3,\ \ldots\ldots,m.$$

(b).The discrete coordinate points for computational plain, shown in figure 4. b.

$$x_i=i\Delta x, \quad \text{for } i=0,\ 1,\ 2,\ 3,\ \ldots\ldots,m;\ \ \Delta x=\frac{L}{m},$$

$$\xi_j=i\Delta\xi, \quad \text{for } j=0,\ 1,\ 2,\ 3,\ \ldots\ldots,n;\ \ \Delta\xi=\frac{1}{n},$$

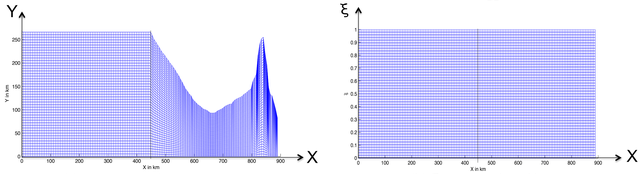

(a). Variable grid of physical plain (b). Regular spacing grid

Figure 4. Variable and Regular grid for domain

4.2 Transformed equations

$$\frac{\partial N}{\partial t}+u\frac{\partial N}{\partial x}+v_\xi\frac{\partial N}{\partial \xi}=\sigma_x\frac{\partial^2 N}{\partial x^2}+\Lambda_\xi\frac{\partial^2 N}{\partial \xi^2}+\Lambda_{x\xi}\frac{\partial^2 N}{\partial x\partial \xi}-(\frac{\alpha(\phi,H,t)N}{K_N+N}-r)P+r_1D+\frac{m_0+\zeta^+(t)}{M(t)}(N_D-N)$$

$$\frac{\partial P}{\partial t}+u\frac{\partial P}{\partial x}+v_\xi\frac{\partial P}{\partial \xi}=\sigma_x\frac{\partial^2 P}{\partial x^2}+\Lambda_\xi\frac{\partial^2 P}{\partial \xi^2}+\Lambda_{x\xi}\frac{\partial^2 P}{\partial x\partial \xi}+(\frac{\alpha(\phi,M,t)N}{K_N+N}-r)P-\frac{p_1P}{A}(\frac{c(A-A_{Th})Z}{K_Z+(A-A_{Th})})-(\frac{\mu P}{k+P})P-\frac{m_0+\zeta^+(t)}{M(t)}P$$

$$\frac{\partial Z}{\partial t}+u\frac{\partial Z}{\partial x}+v_\xi\frac{\partial Z}{\partial \xi}=\sigma_x\frac{\partial^2 Z}{\partial x^2}+\Lambda_\xi\frac{\partial^2 Z}{\partial \xi^2}+\Lambda_{x\xi}\frac{\partial^2 Z}{\partial x\partial \xi}+\frac{ec(A-A_{Th})Z}{K_Z+(A-A_{Th})}-\frac{\zeta(t)}{M(t)}Z-gZ$$

$$\frac{\partial D}{\partial t}+u\frac{\partial D}{\partial x}+v_\xi\frac{\partial D}{\partial \xi}=\sigma_x\frac{\partial^2 D}{\partial x^2}+\Lambda_\xi\frac{\partial^2 D}{\partial \xi^2}+\Lambda_{x\xi}\frac{\partial^2 D}{\partial x\partial \xi}+(\frac{\mu P}{k+P})P-r_1D+\frac{p_1P}{A}(\frac{(1-e)c(A-A_{Th})Z}{K_Z+(A-A_{th})})-\frac{p_2D}{A}(\frac{ec(A-A_{th})Z}{K_Z+(A-A_{th})})$$

$$\frac{\partial F}{\partial t}+u\frac{\partial F}{\partial x}+v_\xi\frac{\partial F}{\partial \xi}=\sigma_x\frac{\partial^2 F}{\partial x^2}+\Lambda_\xi\frac{\partial^2 F}{\partial \xi^2}+\Lambda_{x\xi}\frac{\partial^2 F}{\partial x\partial \xi}-\lambda F+e^{m_r t_r}PP, \quad m_r=-\log(0.04/t_r),$$

Where

$$v_\xi=\frac{1}{b}\left[v-\left(u+\frac{2\sigma_x}{b}\frac{\partial b}{\partial x}\right)\left(\frac{\partial b_1}{\partial x}+\xi\frac{\partial b}{\partial x}\right)+\sigma_x\left(\frac{\partial^2 b_1}{\partial x^2}+\xi\frac{\partial^2 b}{\partial x^2}\right)\right],$$

$$\Lambda_\xi=\frac{1}{b^2}\left[\sigma_y+\sigma_x\left(\frac{\partial b_1}{\partial x}+\xi\frac{\partial b}{\partial x}\right)^2\right], \quad \Lambda_{x\xi}=-\frac{2\sigma_x}{b}\left(\frac{\partial b_1}{\partial x}+\xi\frac{\partial b}{\partial x}\right)$$

5. Results and Discussion

Figure 5 (a), (b) and (c) are showing a definite pattern with time lag around 30 to 90 days between two consecutive trophic level of species. It is obvious that for high growth of prey, predator should be at lower concentration.

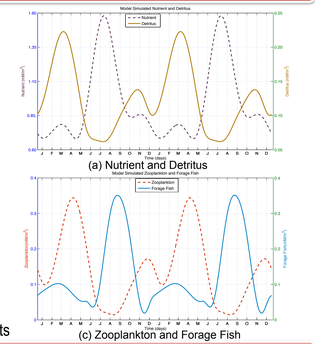

(b) Phytoplankton and Zooplankton

(a) Nutrient and Detritus

(c) Zooplankton and Forage Fish

Figure 5. Model Simulated Results

5.1 Validation

Model simulated phytoplankton is compared with SeaWiFs and Modis Aqua derived monthly mean chlorophyll-a

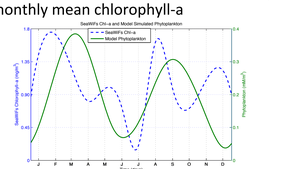

(a) SeaWiFs chl-a and phytoplankton

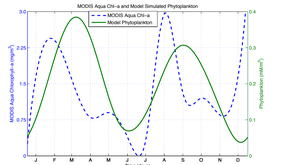

(b) Modis aqua chl-a and phytoplankton

Figure 6. Satellite observed chl-a and model simulated phytoplankton

6. Conclusions

The model simulated results are able to reproduce the trend in the observed data, especially the bimodal oscillations. For further validation, more recent data is needed and also, the model needs to include more species. Coordinate transformations, which are used for numerical treatment of irregular boundary into regular boundary of domain during numerical simulation with higher order of accuracy, are extremely useful in physical – biological studies.

References

1. Chaturvedi, N. (2005). Variability of chlorophyll concentration in the Arabian Sea and Bay of Bengal as observed from SeaWiFS data from 1997–2000 and its interrelationship with Sea Surface Temperature (SST) derived from NOAA AVHRR. I. J. of Remote Sensing, Vol. 26, No. 17, 3695-3706.Reference B
2. Deshkar, S., Lakhmapurkar, J. and Gavali, D. (2012). State of three estuaries of Gulf of Khambhat. Indian Journal of Geo-Marine Sciences, Vol. 41 (1), 70 - 75.
3. Dube, A., Jayaraman, G. and Rani, R. (2010). Modelling the effects of variable salinity on the temporal distribution of plankton in shallow coastal lagoons. J. of Hydro-environment Res., vol. 4, 3: 199-209.
4. Dube, A. and Jayaraman, G. (2008). Mathematical modelling of the seasonal variability of plankton in a shallow lagoon. Nonlinear Analysis 69, 850-865.
5. Evans, G. T. and Parslow, J. S. (1985). A Model of Annual Plankton Cycles. Biological Oceanogr., vol 3, 327-347.
6. Fasham, M. J. R., Ducklow, H. W. and Mckelvie, S. M. (1990). A nitrogen-based model of plankton dynamics in the oceanic mixed layer.J. of Marine Res.,48,59-639.
7. Fasham, M. J. R., Ryabchenko, V. A. and Gorchakov, V. A. (1998). Seasonal dynamics and biological productivity in the Arabian Sea euphotic zone as simulated by a three-dimensional ecosystem model.G. Biogeo. cycles,vol. 12,3:501-530.
8. Ishizaka, J. (1990). Coupling of Coastal Zone Color Scanner Data to a Physical-Biological Model of the Southeastern U.S. Continental Shelf Ecosystem, 2, An Eulerian Model. J. Geophys. Res., vol. 95, no. C11, 20201-20212.
9. Jaiswar, J. R. M., Mandalia, A. V., Narvekar, S. M. and Karangutkar, S. H. (2011). Nutrient Fluxes and Adaptation to Environmental Dynamics by Phytoplankton in the Gulf of Khambhat. I. J. of Curr. Res., vol. 3 (9): 5-13.